Science Robotics
AAAS

# Manuscript Template

## FRONT MATTER

### Title

- An Anthropomorphic Soft Skeleton Hand Exploiting Conditional Models for Piano Playing
- Skeleton Hand Piano Playing

### Authors

J. A. E. Hughes, [1]* P. Maolino, [1] F. Iida[1]

### Affiliations

[1] Bio-Inspired Robotics Lab, Department of Engineering, University of Cambridge, Trumpington Street, CB2 1PZ.
***** Corresponding author, jaeh2@cam.ac.uk

### Abstract

The development of robotic manipulators and hands which show dexterity, adaptability and subtle behavior comparable to human hands is an unsolved research challenge. In this article, the use of the passive dynamics of mechanically complex systems, such as a skeleton hand, as an approach to improving adaptability, dexterity and richness of behavioural diversity of such robotic manipulators, is considered. Using state-of-the-art multi-material 3D printing technologies, it is possible to design and construct complex passive structures, namely a complex anthropomorphic skeleton hand which shows anisotropic mechanical stiffness. A new concept, termed the 'Conditional Model', which exploits the anisotropic stiffness of complex soft-rigid hybrid systems is proposed. In this approach, the physical configuration, environment conditions and conditional actuation (applied actuation) result in an observable 'Conditional Model' allowing joint actuation through passivity based dynamic interactions. Using the 'Conditional Model' approach allows the physical configuration, and actuation to be altered enabling a single skeleton hand to perform three different phrases of piano music with varying styles and forms facilitating improved dynamic behaviors and interactions with the piano over those achievable using a rigid end effector.

### Summary

Conditional Models provides a method of achieving varying behaviors by utilizing hybrid and passive mechanical structures.

## MAIN TEXT

## Introduction

There is increasing interest in the study of nature to provide bio-inspiration for the development of robots with physical and cognitive abilities comparable to biological systems (*1*, *2*). Animals can interact in highly complex and varied ways with rapidly evolving, information-rich environments (*3*). Previous work on biologically inspired robotics has demonstrated that the complexity in animals' behavior results from the reciprocal coupling between the controller (brain), the body and its interactions with the environment (*4*, *5*). Complex behavior does not result from the controller or brain alone, but from a distributed complexity across the entire system including the mechanical body (*6*).

The mechanical properties and design of systems plays a considerable role in the intelligent functioning of animals and machines. This can be observed in passivity-based robot control (*7*, *8*). Passivity can, for example, be used to achieve a pendulum-like swing of legs for locomotion, requiring no explicit active control to achieve stable bipedal walking (*9*). High functioning passively-controlled robots have achieved a range of different behaviors such as robotic swimming, flying and manipulation (*10*). Smart mechanical design enables systems to show exquisite and complex behaviors that are self-stabilizing and energetically efficient at reduced computation cost (*11*).

Achieving functional behaviors through passivity is crucial for the survival of biological systems, however, as a design method for robotic systems, passivity is known to intrinsically restrict the range of behavior (*12*). Underactuated control provides a compromise and can expand the range of behaviors by introducing a coupling between passive mechanics and limited joint actuation (*13*, *14*). This creates behaviors which are highly environmentally dependent and sensitive to changes but limits behavioral diversity, typically with a one-to-one mapping between environment and behavior imposed (*15*, *16*). This limitation can be particularly seen in robotic manipulation and hand design where passive control and underactuated mechanical design allows only a single (*17–19*), or at best, a limited number of behaviors to be achieved (*20–24*). To leverage the intelligence of passive mechanical bodies, a method for generating a range of behaviors in variable environments is required.

Achieving behavioral diversity in robotics, while utilizing passive dynamics, remains a fundamental challenge. There have been several recent approaches using passivity to achieve complex (i.e. varied and adaptive) dynamic behaviours, where the complex behavior emerges from many hard to control independent mechanical components. One approach is to actively control the mechanical dynamics of the robots by implementing variable stiffness mechanisms allowing adaptation of the passive behaviors to varying environments (*25–27*). While this approach allows different behaviors to be achieved, the inclusion of actuators limits the scalability and requires more complex control (28–31). A second approach is the use of materials to alter or adapt the behavior (32). Soft deformable materials can be integrated into robots to expand the diversity of achievable behavioral patterns (33, 34). Behaviors of robots using soft deformable materials are generated through the mechanical dynamics of interactions between the environment and materials (35). The increased compliance of the soft materials provides more flexibility, enabling a wider variety of mechanical dynamics. However, the inherent flexibility of soft

materials can result in behaviors which are ill-defined and highly variable. A key challenge therefore, is controlling the mechanical compliance when using softer materials (36, 37). This has been demonstrated with soft robots using variable-stiffness materials to achieve a range of movements and to modulate interactions with the environment (38–40). The synergy between soft bodies and actuation methods can then be utilized. This allows the movement of soft bodies to be limited or constrained, in turn limiting the requirement for complex additional actuation sources. In particular, work on adaptive synergies (41–43) and tendon routing (44) shows significant breakthroughs and developments with respect to robotic manipulators. Although many of these approaches provide methods for exploiting mechanical passive dynamics, they do not provide a framework for significantly scaling complexity and diversity in behavior.

This paper proposes an alternative approach, using hybrid soft-rigid mechanical structures, where the stiffness of the structures can be set heterogeneously across the body. This builds upon well understood techniques such as flexure joints which utilize anisotropy (*25*, *54*, *55*). By taking advantage of state-of-the-art multi-material 3D printing techniques, complex hybrid mechanical structures can be constructed (45–47). Given appropriate environmental and actuation conditions, this heterogeneity of stiffness can be exploited, with the conditions restricting the joint space such that the observed model of the structure, termed 'conditional model', varies (Fig. 1). In addition to the conditional actuation applied to the system, there is a second observable actuation, the joint actuation, which determines the passivity based dynamic interactions of the system. The passive interactions arising from the joint actuation may lead to a change in the physical configuration of the structure altering the Conditional Model (Fig. 1B). This approach provides both a conceptual understanding of how complex behaviours can emerge from a passive based hybrid structure whilst also informing the design and control necessary to achieve different Conditional Models and accompanying behaviours.

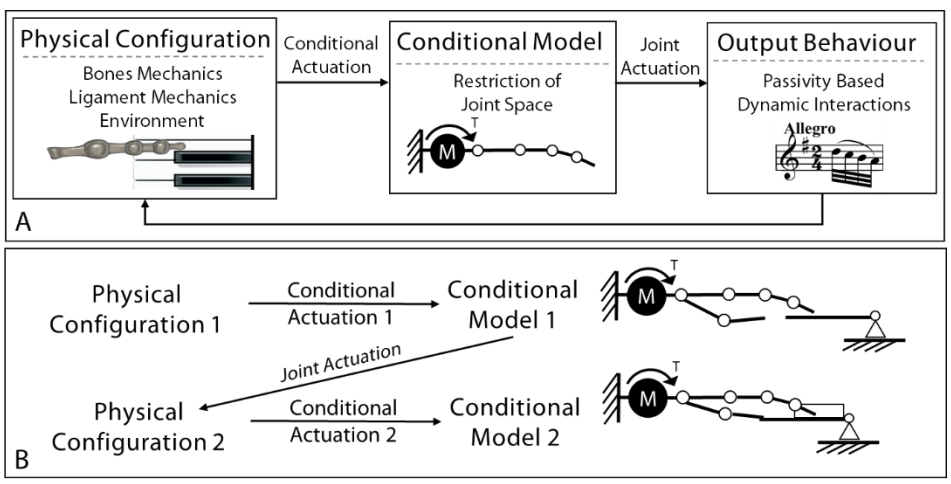


**Fig. 1. Representation of the Conditional Model.** (**A**) A Conditional Model occurs when a conditional actuation is applied to a physical configuration (e.g. geometry and materials). This model represents the interaction between the system and the environment. There is a secondary internal actuation of the system, the joint interaction, which is dependent on the restriction of the joint space of the conditional model. This results in the passive based output behavior leading to a change in the initial physical configuration of the system. (**B**) For each resultant conditional model, the joint actuation is dependent on different physical configurations from which a second conditional model can be achieved. In this way, it is possible to achieve Conditional Models which then allow other Conditional Models of emerge.

The ability of a system to show many Conditional Models enables diverse and complex mechanical dynamics from a single system. This mirrors how the human hand can show highly varied dynamics, for example a strong fist can be formed to hit a rigid wall, or a soft finger can be used to touch a smooth surface. The range of Conditional Models which can arise from one passive structure is dependent on the mechanical design, actuation and environmental conditions. Certain conditional models can only be achieved by first triggering previous conditional models and associated output behaviors, hence a typical one-to-one mapping of control inputs and behavior can no longer be used (Fig 1B).

This article investigates the behaviors achievable through the emergence of Conditional Models. The mechanical complexity of structures, in this case the many interacting mechanical parts with varying stiffnesses, plays a crucial role in the emergence of Conditional Models. The complexity enables adaptive environmental interactions, yet also allows the emergence of specific conditional models and behaviours. The greater the variety of mechanical dynamics within the body of a robot, the wider the variety of Conditional Models which can be determined through different physical configurations and actuation conditions. Mechanical behavior is bounded by the physical design and geometry of the system, for example, the joint design and the material properties whilst the environment and surroundings impose conditions on the complex mechanical system contributing to the behavior (*41*, *52*, *53*). This approach to design and control a mechanical body leads to richer behavioral diversity in comparison to the previously discussed passivity-based and soft robotic approaches. The diversity of behavior originates from the complexity of the mechanical design, whilst simultaneously reducing the complexity of the required control. To demonstrate this concept, a 3D printed anthropomorphic robotic hand interacting with a complex environment is considered. Existing anthropomorphic hands often require complex actuation,or oversimplify the model such that complex joint behaviors are lost (*48–51*). In this work, we present a new approach to producing near exact replication of human bone and ligaments by 3D printing, with the behavior dominated by passive dynamics.

To validate the proposed approach, a case study of the dexterous robotic hand playing a piano is presented. Piano playing emerges through the coupling between the biomechanics and neuromuscular dynamic of the pianist (mechanical impedance of the finger) and the dynamics of the piano itself (*56*). Piano playing thus relies on the interaction between the environment and the mechanics of the players' hand. Piano playing robotics research dates back to the 1980s (*57*), with many piano playing robots developed with a focus on both the mechanical and algorithm development (*58–62*). Most of the robots utilized rigid finger joints with no compliance such that a high accuracy of finger positioning can be achieved. However, the control required to achieve a variety of more nuanced playing styles, ranging from highly precise rapid movements to softer more adaptive playing, has not been explored thoroughly. Successful expressive and varied piano playing within the fixed environmental conditions provided by the piano poses a rigorous test for the Conditional Model framework and robotics in general and demonstrates the contributions of this concept to the research community.

## Results

### *Designing Internal Conditions: Anthropomorphic Soft Hand Skeleton*

The process of designing and building systems with anisotropic stiffness which allow a range of different 'Conditional Models' requires a different approach to that of building conventional rigid actuated systems, and is more challenging. Biological systems show a

diverse range of complex joints, including highly mobile joints such as the shoulder of hand joints. These provide an excellent starting point for the design of joints which show anisotropic stiffness and can have many different observable modes (*63*). The combination of bone-bone interactions and ligaments creates complex passive behaviours (*64*, *65*). Unlike pin joints typically used in conventional rigid robotic systems, these structures can exhibit anisotropic behaviors depending on the actuation applied and the environmental interaction. For this piano playing case study, an anthropomorphic hand which utilizes these complex interactions is developed. The design of physical system (the physical configuration) focuses on the joint design and material properties of the hand skeleton.

Fig. 2A shows the model of the anthropomorphic hand skeleton used. This is directly inspired by human anatomy with bones and ligaments placed as they are in nature (*66*). Every finger joint is encapsulated by ligaments constraining the movement and stiffness of the joint allowing the two bones to move independently and to interact. Unlike many other anthropomorphic robotic hands this allows both osteokinematics, observable movement of bone shafts and also anthrokinematics, movements at joint surfaces which cannot be directly observed and are considered to be passive (*67*). By 3D printing this model with varying ligament stiffness, the anisotropic properties of the finger can be varied (Fig. 2B). By printing joint ligaments with sufficient compliance, the anisotropic stiffness allows for complex behaviors influenced by external actuation and interaction with the environment. Video S1 shows the multi-material 3D printing process and the flexibility and range of movement of the printed hands.

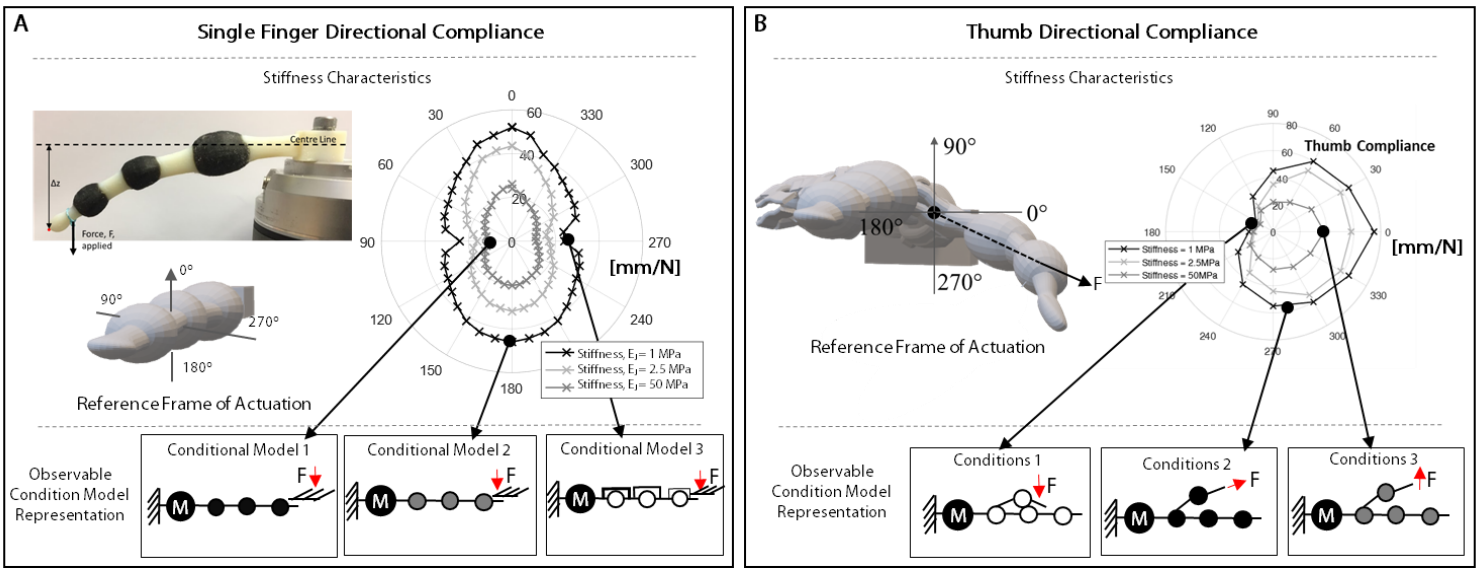


**Fig. 2. The Piano Playing Hand.** (**A**) Anthropomorphic model of the hand used showing three groups of ligaments which influence the three behavior primitives investigated. (**B**) The 3D-printed hand conditional stiffness system attached to the UR5 robot arm which provides the external actuation and the piano environment used.

Fig. 3A shows the experimentally determined stiffness of a 3D printed index finger when force is applied perpendicular to the finger-tip at varying orientations. A static force was applied to the finger-tip whilst the metacarpus was fixed, allowing the overall perpendicular stiffness behavior to be measured. Three different materials (Young's Modulus $E_J$ of 1, 2.5, and 50MPa) were used to print the ligaments (see more details in the

Methods Section). As shown in Fig. 3A, varying the physical configuration (ligament stiffness) or the environmental conditionals (angle of force applied) can give rise to different observable models which provide different output behaviours. Due to the geometry of the bones and the interactions between the bones and the ligaments, the stiffness is greater in the ventral-dorsal direction in comparison to the lateral direction. In particular, lower compliance is observed in the horizontal plane where it can be observed that lateral movement leads to a 'jamming' between the two bones limiting the compliance of the joint in that direction (*68*). The stiffness is not completely symmetrical around the vertical axis, reflecting the non-symmetric bone-bone interaction when the heads of the bones interact. Thus, for different conditions, the Conditional Model of the system can be observed to have changed.

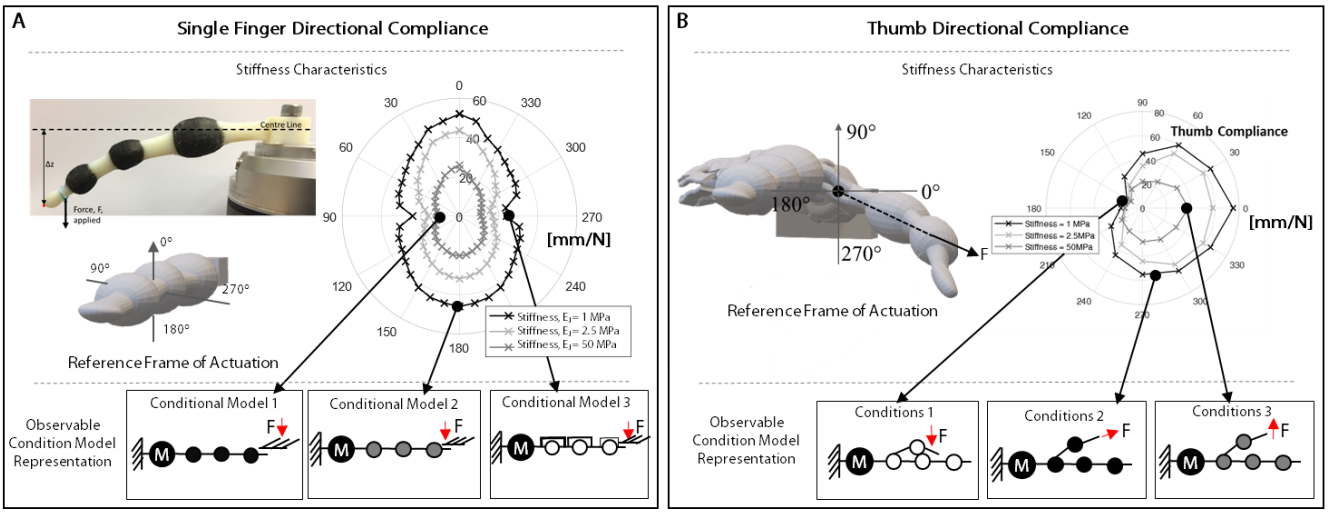


**Fig. 3. Demonstration of the Conditional Model.** (**A**) Single finger compliance behaviours of a single finger (distal phalange to metacarpal) printed to scale with varying ligament stiffnesses. This allows the emergence of different conditional models for single finger interactions. (**B**) The directional compliance of a thumb. It is shown how the different environmental interaction and physical configuration leads to the emergence of different Conditional Models.

Similar to the stiffness deformation landscape of a single finger shown in Fig. 3A, the anisotropic nature of the thumb stiffness shows similarly diverse and complex behaviors, with a larger range of different possible Conditional Models. Behavioral diversity of this finger can be generated by exploiting the variable conditional models imposed by the environment, actuation and physical constraints. A similar design strategy can be applied to the other parts of the complex hand skeleton. The thumb joint is more complex and allows similar exploitation of anisotropic stiffness; the larger number of ligaments contribute to the directional stiffness allowing a much greater range of arthrokinematic behavior as shown in Fig. 3B. The different conditional models that can be achieved with the thumb joint are more complex and show greater variation than those possible with a single finger.

The ligaments in the skeleton model are grouped into three types (Fig. 2A), those that contribute to finger joint stiffness, span stiffness and thumb abduction/adduction stiffness. The material properties of these ligaments are denoted by $E_J$, $E_S$, and $E_T$ for each group respectively. The material property of these ligaments controls the stiffness of these joints influencing the overall behaviors of the passive hand;. As demonstrated in Fig. 3A, the collateral ligaments and other associated finger ligaments contribute to the anisotropic

stiffness, and hence conditional models of the finger which can be controlled by varying the material property $E_J$. The variable span stiffness is controlled by the deep transverse metacarpal ligaments which is determined by the material property $E_S$. Finally, the stiffness of the complex thumb joint and the range of motion is controlled by the material stiffness ($E_T$) of the palmer carper-metacarpal II ligaments and surrounding ligaments.

To 'engage' the anisotropic stiffness and select a specific Conditional Model, an active component to provide external actuation to the passive system is needed. In this case study, a multi-degree of freedom UR5 robotic arm was used to provide wrist actuation with the passive hand attached to the arm (Fig. 2B). The wrist actuation allows for dynamic changes in hand position with respect to the environment. This promotes varying interactions and dynamic coupling between these two components allowing different Conditional Models to be observed. Fig. S2 shows the overall architecture used to demonstrate the case study.

To experimentally determine how the physical configuration and environmental interaction impose restrictions on the joint, and thus determine the joint actuation from specific conditional actuation, experiments investigating the influence of material properties on piano playing behaviors have been undertaken. Within these experiments, the coupling between the mechanical system and the environment is investigated by varying the wrist dynamics and material properties of the hand.

***Analysis of Conditional Model Concept for Behavioral Diversity***

To allow systematic analysis, we investigate three behavior primitives: single finger tapping, thumb adduction/abduction, and hand span behavior. The combination of these primitives enables a wide range of playing behaviors and different Conditional Models. These three behavior primitives map to three ligament groups for which the material properties are varied: fingers joints ($E_J$), thumb ligaments ($E_T$) and span ligaments ($E_S$).

*Single Finger Behavior*

The single finger exhibits a wide variety of conditional models and hence behaviors depending on the conditions provided. The first series of experiments involves a single finger playing a single note, 'tapping' one piano key where wrist actuation is only applied in the vertical plane. Considering a right-handed reference frame centered on the wrist with the z axis vertically upwards, this corresponds to wrist movement in the z axis. The control parameters of this wrist actuation include the frequency (or playing speed) and the displacement of vertical motions. For different control parameters the output frequency, rate of force applied and the maximum force at the finger-tip in contact with the surface of piano key are observed. The focus of this analysis the ability of the internal conditions to control the overall performance of piano playing with one finger. In particular, the change in output behavior for fingers with varying ligament stiffness was analyzed. Four single fingers were tested, each 3D-printed with ligaments ($E_J$) of different Young's Moduli.

Fig. 4A (left plot) shows the input-output frequency response of the finger, which is an important metric when considering the achievable tempos when piano playing (*69*, *70*). The range of output frequency in each finger was measured by actuating the wrist vertically, oscillating with a fixed amplitude in the z axis. When increasing the input frequency, the output frequency of the rigid finger can be considered to be the same as the input frequency within the range of reasonable playing frequencies. The range of

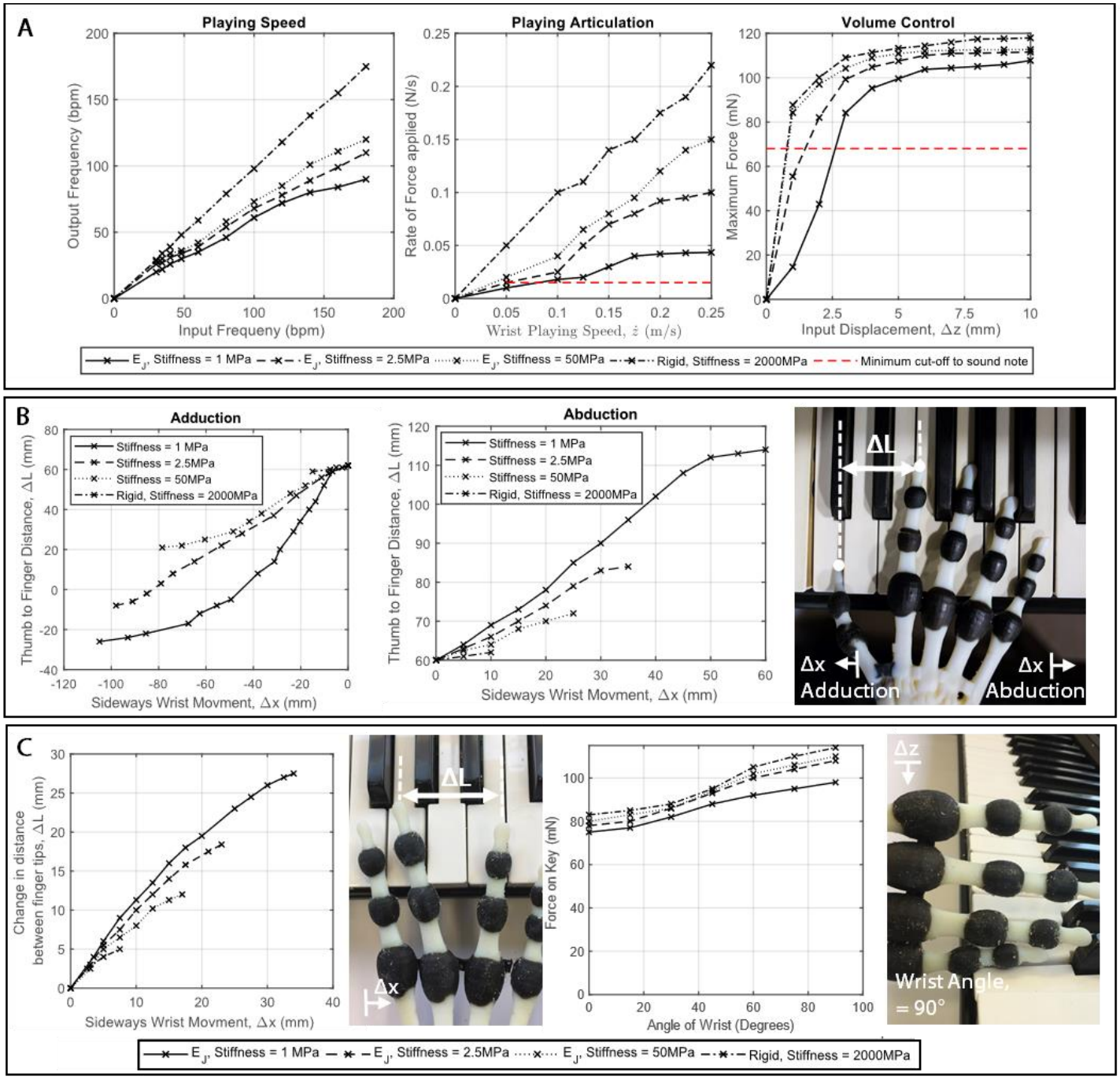


**Fig. 4. Experimental Testing of Behavioral Primitives.** (**A**) Single Finger playing experiments with 3D printed fingers with varying material stiffness ($E_J$) showing the effects of varying different control parameters: frequency of playing (playing speed), rate of note playing (playing style, e.g. legato/staccato) and the maximum force detected on the finger tip (volume). The force was measured using FSR on the piano keys. This highlights the different in joint actuation for the different models. (**B**) Abduction/Adduction distance measured between the tip of the thumb and the tip of the first finger when wrist is actuated horizontally after the thumb is moved vertically down such that it is pressing the key. Experiments were undertaken with hands with varying thumb ligament stiffness ($E_T$). (**C**) Hand span stiffness demonstrated with a single finger (left) where the displacement between the second and third finger is measured with the second finger playing a note and the wrist actuated horizontally. Whole hand playing (right) when the wrist is actuated at varying amounts and the stiffness changed. The figure shows the varying output force when these conditions are changed.

conditional models which the rigid finger can achieve is low, whilst for the more compliant fingers, which exhibit a more complex and non-linear relationship between the conditional actuation and the joint actuation, a greater range of models is possible. As the stiffness of the ligaments is reduced, the anisotropic stiffness is such that the system shows some non-linear behavior, with the damping effect limiting the maximum achievable frequency. Lower stiffness fingers experience lower frequency environmental interaction and a different conditional model is achieved in comparison to the high stiffness finger. By lowering the stiffness, the conditional model has a limited range of playing frequencies in comparison to the fully rigid finger where the model is capable of playing music with a greater range of frequencies. However, a stiffer finger has a smaller range of different Conditional Models resulting in a trade-off of other playing capabilities and stylistic behaviors.

Fig. 4A (middle plot) shows the rate of tapping force at the contact to the piano key with respect to different frequencies (or actuation speeds). The rate of tapping force indicates the articulation of sound, which directly influences the transition between notes ranging from slurred/legato to staccato. The lower rate of force change results in smoother transition between two notes. This experiment highlights the salient differences between the rigid and softer, compliant fingers. Although rigid fingers can achieve a conditional model which exhibits a larger range of force changes for a greater range of input frequencies, they cannot achieve lower playing rates, especially at a higher frequency. These results indicate that a soft finger is necessary to play fast slurred or legato pieces, as it provides more suitable conditional models, while a more rigid one should be employed for an articulated music.

Similar behavior characteristics can be seen for the peak force when playing using a single finger, which indicates the volume of note. Fig. 4A (right plot) shows that a rigid finger can generate a larger variety of peak forces, while the subtle control of volume could be easier when a softer finger is used. The results demonstrate that the mechanical properties of the piano affect the achievable conditional model, limiting the ultimate ranges of the behavior. Actuation can be used to trigger a given conditional model and hence behavior or response within these limits by the physical limitations of the system.

These results highlight the various trade-offs between different stiffness finger ligaments and actuation combinations. It is shown how anisotropic stiffness can be exploited through the physical configuration and environmental interaction to enable specific Conditional Models. There is no unique combination of actuation and mechanical properties for one Conditional Model, behavior or playing style. However, the choice of the physical configuration (geometry and materials) does limit the range of behaviors that can be achieved. Video S2 highlights the range of movement of a single finger, showing the finger trajectory and tone when playing a single note with fingers of different joint stiffnesses.

*Thumb Adduction/Abduction Behaviours*

For these experiments we specifically focus on the thumb and index fingers as they exhibit a rich variety of motions in comparison to other human hand movements, with high mechanical complexity providing a large range of Conditional Models. The thumb abduction and adduction movement are particularly interesting as the range of movements and behavior reflects the complexity of the thumb anatomy and provides a great deal of

functionality for hands (*71*), and more specifically for piano playing. Video S3 demonstrates the abduction/adduction behavior which can be achieved with the passive hand structure when using the coupling between environment and actuation. To achieve these abduction/adduction behaviours it is necessary to pass through specific conditional models which enable other conditional models to be observed.

In this experiment, finger movement was articulated into two phases: first, the wrist was actuated downward in the z axis with a certain stroke and a fixed speed such that the thumb finger-tip could press the key down all the way. Secondly, the wrist was then moved horizontally to the keys in the x-axis such that the index finger is moved over the thumb. It is important to note that the thumb abduction behavior is possible because in the previous conditional model, the thumb finger is prevented from moving sideways by the neighboring key during the second movement. In this way the actuation is used to achieve different Conditional Models, and through these it then possible to access other models, showing some emergence of different conditional models. After these wrist actions, the horizontal distance between thumb and index finger tips is measured as an indication of the adduction/abduction behavior of the hand. This type of behavior is used by human players to allow smooth transitions when moving sequentially over notes, for example in scales or when performing jumps and rapid movements (*72*).

As in the single finger experiments, we investigated the effect of ligament material properties on the behavior of the hand. Only the material properties of the adduction/abduction ligaments were varied whilst keeping the others the same. Fig. 4B shows the distance between the two fingers with respect to different horizontal displacement of the wrist joint for four different thumb ligament stiffnesses, $E_T$, ranging from 1 MPa to 2GPa.

When rigid ligaments were used, the two fingers have a limited ability to move relative to each other when horizontal displacement is applied to the wrist. Thus, when the wrist is moved the maximum adduction distance was found experimentally to be approximately 18mm, with the thumb only able to move on the pressed key until the neighboring key prevented further movement. In contrast, when decreasing the stiffness of the ligament, the maximum adduction distance can be significantly extended, with over 80mm adduction seen with the 1MPa ligament enabled by a significantly different conditional model. As the key width of ordinary piano is 13mm, the ligament stiffness can influence the capability of playing between 5 keys with abduction. The softness of the ligament also influences the nonlinear relationship between the wrist movement and the abduction distance due to the complex bone-ligament interactions. The softer the ligaments the greater the non-linearity of the abduction behavior of the thumb joint and the lower the horizontal displacement required to achieve a given range of abduction. For these softer ligaments there is a more complex, non-linear relationship between the conditional actuation and the joint actuation, with greater differences between different Conditional Models. These results show how different behaviours can emerge from different Conditional Models, with some behaviors only able to be achieved from specific Conditional Models.

A similar behavior is observed for thumb abduction. The rigid ligaments provide limited abduction with the distance again determined by the piano keys. The lower stiffness ligaments allow over 50mm of extension between the thumb and finger with the 1MPa ligaments. The greatest non-linearity is also seen with the lower stiffness ligaments with

the maximum abduction limited by the physical mechanics of the specific Conditional Model providing a limitation of the joints in the conditional model.

*Hand Span Behavior*

The next experiment considers the ability of the hand to compress/stretch laterally allowing passive translation and rotation the fingers. This allows the fingers to stretch laterally enabling jumps and smooth transitions, with the length of jumps between notes able to vary. Additionally, the translation of fingers allows the hand to be rotated such that the fingers are playing on the side, with the whole hand contributing to the note playing. Designing a passive anthropomorphic skeleton for these tasks is more challenging as a larger portion of the hand is involved in this behavior. The finger joints, $E_J$, contribute to this hand behavior, however, the deep transverse metacarpal ligaments (labelled as hand span stiffness) provides additional stretch and are the determining factor in the behavior of this primitive.

The ability of the fingers to move laterally, enabling smooth sideways transitions between notes and sideways note playing is now considered. Similarly to the previous experiments, the hand stretch behavior can be achieved by a two-phase articulation of wrist actuation. Firstly, the wrist is actuated downwards in the z axis by a given amount at a given rate so that the key is fully pressed with the second finger with sideways movement limited due to the piano keys which remain un-pressed. The wrist is then actuated horizontally such that the finger is moved laterally, with the key kept pressed down such that the angle of the finger to the hand varies depending on the span stiffness. Again, two different consecutive Conditional Models are used to achieve a specific behavior. A series of experiments were conducted using four 3D printed hands with different span ligament stiffness ($E_S$): 1MPa, 2.5MPa, 50MPa and 2GPa. The horizontal displacement between the second finger and the middle finger is measured. It is important to note that, for all these experiments, the finger ligament stiffness ($E_J$) was kept lowest possible at 1MPa to make the largest stretch possible. The measurement of lateral displacement for the four hands is shown in Fig. 3C (left), where the stretch is measured at every 5mm increment of sideways movement. Video S4 shows how compression in the span of the hand can be used to achieve jumps of varying length and how angled hand playing can be used.

The hands with the 2GPa and 50MPa hand span stiffness exhibit very small displacement under 10-20mm most of the time, with limited change in the Conditional Model. As the stiffness is reduced the stretch range increases significantly, with a maximum recorded stretch of over 40mm. The response is initially linear, however for lower stiffness the response of the ligaments becomes increasingly non-linear as material and geometric constraints are reached and the range of the joints is restricted, resulting in a different Conditional Model. Varying the stretch ligament stiffness significantly affects the range of lateral movement possible with a single finger, as there is a physical limit on the movement of the finger joint.

This span stiffness also influences whole hand playing, more specifically little finger playing where the wrist is at an angle to the piano (Fig. 4C right picture). When playing chords with jumps whole hand playing if often used and the hand can be angled to achieve playing of different styles. Here the span stiffness dominates the playing behavior. The key force is investigated when the hand is actuated downwards by 15mm pressing the key for different wrist angles. When the hand is perpendicular to the piano key the force is the

highest as the span stiffness is fully engaged and acting in full compression. At lower angles the stiffness is lower, often significantly so. The increase in force with angle is far greater for the stiffer span stiffness, with an increase of over 30mN. Varying the angle of interaction and span stiffness affects the force which can be applied to the piano keys and allows different Conditional Models to emerge.

***Utilization of Conditional Models for Complex Piano Playing***

The previous experiments have shown how Conditional Models for one or two finger can be achieved. The next challenge is how to integrate these individual Conditional Models mechanisms to create a robot with significantly increased range of behaviors. This integration challenge is difficult as some of the physical and actuations conditions necessary for certain behaviors can interfere or are not compatible with others. The integration process is not simply the aggregation of individual mechanisms; Conditional Models cannot always be treated in an additive manner. The resultant behavior is dependent on the interactions between the different sub-systems. Therefore, a consideration is to avoid conflicts of conditions while integrating the required behaviors without compromising behavioral performances. In the following experiments we present a case study in which such decoupling of conditional models can be used to achieve a range of complex piano playing behavior.

The case study considers the design of an anthropomorphic skeletal hand that can play three different pieces of music without changing the mechanical and material properties (Fig. 5). The first piece is the four bars of 'Toccata' by Scarlatti. This is a fast-paced melody, where single note staccato playing is repeated, with periodic shifts in pitch. The second phrase of music was selected from 'Alligator Crawl' by Fats Waller. This requires consecutive smooth playing of notes an octave (8 notes) apart with a shift between each octave played. The final phrase of music is from 'Rhapsody in Blue' by Gershwin, the archetypal 'glissando' (rapid slide of thumb finger between consecutive notes), which requires thumb abduction smoothly and rapidly sliding over piano keys. Each of these musical phrases required a number of different patterns and combinations of Conditional Models.

To play these pieces in a style similar to humans, the stiffness requirements of different parts of hand for each of these three pieces must be identified. The first piece, 'Toccata,' requires a high frequency and high force staccato playing style, which generally requires a Conditional Model with a high stiffness in the finger as lower stiffness cannot convey high-frequency strong actuation to the keys. Fig. 5A shows the force profiles measured through a sensor attached to a key, to compare the trajectories when the material stiffness of finger joints is varied. The force was measured over 20 cycles to allow variations and deteriorations to be observed. Compared to an experienced human piano player (see the dotted red line), the stiffer finger with 50MPa ligament exhibits the performance closest to ground truth, human playing, whereas the softer fingers (2.5MPa and 1MPa) could not reach the sufficient strength and articulation with adequate temporal length. Therefore, for playing Toccata, it is necessary to have a single finger with the higher stiffness (50MPa) material for the finger joint ligaments to achieve the higher stiffness Conditional Model. It is important to note that due to the material surrounding the single finger performing the playing is critical. To limit playing or interaction of surrounding keys, we wish to maximize the stiffness of the playing fingers whilst lowering that of the surrounding

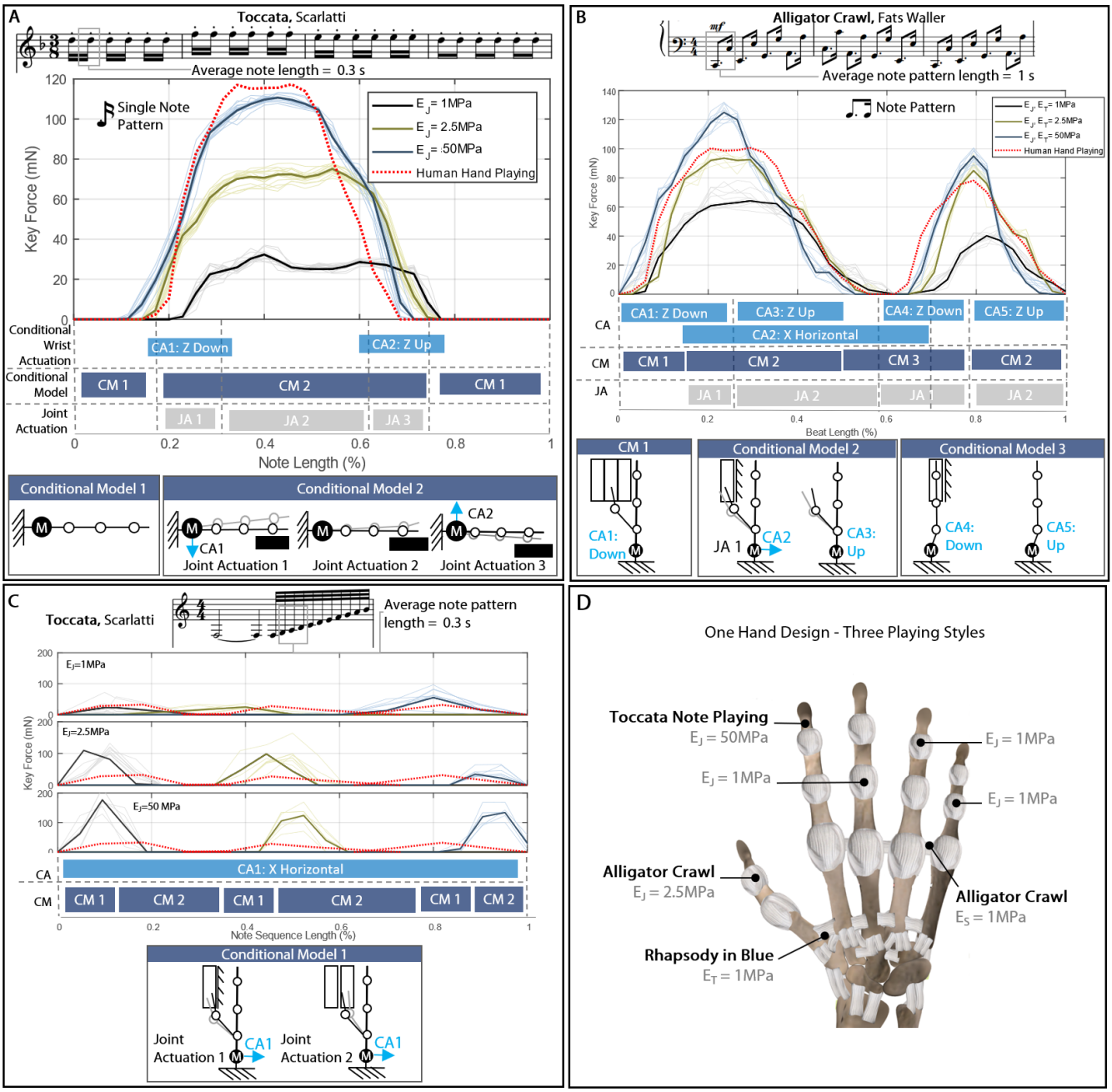


**Fig. 5. Case study demonstrating playing three musical phrases.** (**A**) Results from playing Toccata with a staccato style. Shows the key force for a human playing and robot playing using the second finger for hands with varying stiffnesses. Shows the average response (solid thick lines) and individual force profiles (thinner lines) for varying finger joint stiffness $E_J$ of the finger joints. Shows the repeated musical pattern which forms the basis of this phrase. Representations of the approximate Conditional Models with the Conditional Actuation and joint actuation are shown. The robot playing was repeated 20 times. (**B**) Results from playing the two notes which form the basis of the Alligator Crawl refrain. Shows the response from the force sensors measuring the thumb force which is used to play the first note, and the little finger used to play the second note for different stiffness for all joints ($E_J$, $E_S$, $E_T$). Includes the conditional models and both conditional and joint actuation. The robot playing was repeated 20 times. (**C**) Force sensor results for playing the Glissando (slurred section) in the Rhapsody in Blue phrase of music. Shows the average force sensors results over three keys forming part of this slurred section played with the thumb using hands of different stiffness parameters $E_T$. Show the different Conditional Model states used to achieve the playing behavior. The robot playing was repeated 20 times. (**D**) The stiffness parameters required for the various components of the hand in order to play all three phrases of music closest to that of human playing.

fingers. This highlights how the environment and mechanics of the hand are coupled together, and Conditional Models can be utilized to achieve varying outputs.

The second phrase of music from 'Alligator Crawl' by Fats Waller requires a low hand-span stiffness to allow sideways translation of the finger to achieve the octave spread. Conversely, it is also important to keep these fingers sufficiently stiff to achieve reasonably well articulated notes, to minimize the pause between notes. This requires a complex conditional model which shows variation in the stiffness of different joints. To verify these requirements, we printed three hands with different thumb finger stiffness ($E_T$ of 1MPa, 2.5MPa, and 50MPa) while keeping the hand span stiffness at 1MPa, and measured force profiles exerted on two keys when two consequent notes were being played. Fig. 5B shows the experimental results compared to the force profile of human player. This demonstrates how for the same Conditional Model different joint actuations can be achieved. The lower finger stiffness with 1MPa shows poorly defined notes, leading to slurred and weak articulation. The 2.5MPa finger stiffness, in contrast, shows the closest similarity to the human's. The height and length of the two notes are similar, and there is a comparable pause in between.

The final piece, Rhapsody in Blue, requires rapid succession of playing, with a slurred transition between notes achieved by the thumb finger sliding over the string of notes showing adduction like behavior. To achieve a smooth transition similar to humans, the thumb abduction/adduction stiffness is set appropriately. While the wrist is moving horizontally, the thumb finger needs to interact with consecutive keys in a smooth and repetitive manner, resulting in a set of soft slurred sounds. In this case with consistent actuation, the environmental interaction leads to different Conditional Models and joint actuation. Again, three printed hands with different thumb abduction/adduction stiffness (1MPa, 2.5MPa, and 50MPa) were used in the experiment, where force profiles over three piano keys were recorded. Fig. 5C shows that the thumb abduction stiffness with 1MPa has a temporal force profiles comparable to those of human player, while stiffer joints resulted in less smooth force profile with larger articulated forces.

By combining the optimal joint material required for each of the three phrases of music, a single hand can be printed which allows all three phrases to be played (see Fig. 5D). The thumb must be low stiffness (1MPa) to allow abduction when playing the glissando, and a relatively low span stiffness should be used (2.5MPa). The finger used to play the single notes in the Toccata (the first finger) must be high stiffness (50MPa). Additionally, the joint stiffness of the thumb and little finger must be 2.5MPa to allow sufficient articulation to play Alligator Crawl. All remaining fingers (index and fourth finger) are kept low stiffness (1MPa), such that the other fingers interact preferentially with the piano. For this case study, the three different stiffness requirements were mostly complimentary and the complex nature of the hand skeleton allows varied stiffness to be achieved across one physical model. The actuation conditions required to achieve the playing of these phrases of music is detailed in Fig. S6-S10. A single 3D printed hand playing the three phrases of music is shown in Video S5 with further details of the actuation given in Table S2 in the Supplementary Materials.

## Discussion

Despite extensive robotic manipulation research for the last half century, dexterous hand manipulation remains an unsolved research question. Many of todays advanced robots are

not capable of manipulation tasks which small children perform with ease. We hypothesize that complex passive mechanical structures can be used to address this gap in capabilities. Biological systems utilize mechanical design of bodies to achieve a wide variety of behaviors and thus this should be reflected in manipulation research. Recent advances in multi-material 3D printing technology, allows systematic investigation of the complexity of passive mechanical structures. This approach allows the printing of a passive anthropomorphic hand which provides the ability to reproduce complex human hand capabilities, i.e. various piano playing techniques, to show hand behaviors which cannot be seen by other conventional robots. Most notably this includes the ability to achieve thumb abduction/adduction to perform jumps when piano playing. The utilization of the environment and physical conditions to achieve this makes this technique highly applicable across the robotics field.

Piano playing has proven to be a complex and nuanced challenge requiring a significant range of behaviors and playing styles. It is a challenge which demonstrates how the physical configuration (mechanical geometry and material properties) and system level actuation (wrist actuation) can be coupled with the environment (the piano) to achieve playing of a variety of styles, through the emergence of different conditional models. This approach has enabled robotic piano playing which has a fluidity and range of behaviors which has previously not been demonstrated in robotic piano playing work (*58–61*). While this work investigated only piano playing, the Conditional Model framework is transferable to other applications, especially to those which require diverse dynamic interactions with complex physical environment under severe restrictions of employing sensory motor feedback. We have presented the first steps towards clarifying the role of actuation in complex soft-rigid hybrid systems.

The introduction of soft material elements to robotic systems is particularly important when designing complex passive mechanical structures. The same principle can be applied to robotic systems and manipulators. Continuum deformable bodies have the potential to generate large varieties of behaviors, however, to generate useful and controllable systems a new design methodology is required to unleash the potential. The inclusion of lower stiffness ligaments in the hand design has demonstrated the advantages of softer materials. Using 'hybrid' soft-rigid mechanical systems with 3D printing technologies has enabled the design and fabrication of structures with anisotropic stiffness properties. In addition to the use of soft-rigid materials, the concept of Conditional Model provides a method of utilizing the complexity provided by such structures. The combined conceptual approach and manufacturing technique opens up new exciting directions and methods of research.

The concept of Conditional Models provides an insight into how such anisotropic soft-rigid hybrid structures should be systematically investigated and designed. It provides a framework which identifies the three underlying components necessary for the Conditional Model approach: physical configuration, actuation and environmental conditions. All of these must be considered to achieve a specific Conditional Model which enables passive dynamics interactions in soft-rigid hybrid structures. If these conditions are exploited adequately, a passive mechanical structure can achieve complex piano playing. Such exploitation is largely dependent on the complexity of mechanical structures, which maximizes the range of possible Conditional Models which can emerge and is possible due to state-of-the-art multi-material 3D printing technology.

The research presented in this article can also inspire biological research, in which we can gain understanding of the biological nature of dexterous manipulation by building bio-inspired robots. An obvious criticism might arise from the oversimplification of the anthropomorphic skeletal structure when compared to the biomechanics of human hands when piano playing. There are a number of discrepancies in the playing mechanisms (for example, our system didn't consider the roles of muscle activities and skin frictions etc.). Despite this, the proposed approach allows investigation of the underlying principles of skeletal dynamics to achieve highly challenging manipulation tasks. Previous work has stated that the sound produced by the piano emerges through the coupling between the biomechanics and neuromuscular dynamic of the pianist (mechanical impedance of the finger) and the dynamics of the piano itself (*56*). Piano playing thus relies on the interaction between the mechanics of the piano keys and the players' hand, which can be studied further by using the proposed system.

The proposed architecture can be extended to other application and research directions. The role of the physical configuration should be more thoroughly investigated to analyze the limits of what passive mechanical systems can achieve. In particular, automation of the mechanical design process would enable a more scalable and consistent approach. Another promising area of future investigation is identifying how passive properties can be used to selectively choose a specific environment, and through that, vary the Conditional Model. A key challenge is the integration of active stiffness control, sensory feedback, and motor learning to closer mimic biological systems. Although these advanced motion control capabilities are important, the underlying mechanical complexity enables passive behaviors 'for free' and thus the exploitation of this is the most important consideration.

## Materials and Methods

The case study outlined in this paper demonstrates how Conditional Models can be used to achieve a broad range of behavioral outputs with limited control input presenting materials and methods for producing such systems. The production of the robotic system uses novel 3D printing techniques to allow the printing of variable stiffness complex systems such as the anthropomorphic hand used in this case study. The mechanical design of this hand model, the enabling 3D printing methods, the integration of the full robotics system and details of the experimental methods are provided in this section.

### *Anthropomorphic Hand Skeleton Design*

The anthropomorphic hand skeleton was adapted from a commercial 3D model purchased from TurboSquid (https://www.turbosquid.com). The model has been used as the initial basis for the hand mechanical structure, with various modifications such as changes in material stiffness however we kept changes to be minimum. Starting with an anthropomorphic CAD model of the full hand and wrist including bones, ligaments, tendons and muscles, the tendon and muscles were removed to leave just the passive dynamical system which is formed from the coupling of the rigid bones and more flexible ligaments. The ligaments surrounding the fingers joints (the collateral ligaments) were adapted to simplify the joints and provide increased stability and robustness. The remaining hand model was kept fully anthropomorphic to allow the mechanics of the joint interactions to be fully explored and exploited. To allow the materials of individual parts of the CAD model to be set individually, the CAD model was made such that all parts were uniquely separable. The specific material properties of each bone and ligament can

be set individually allowing control of the internal conditions of the hand. More details of material properties employed are shown in Supplementary Materials.

### *3D Printing*

Multi-material fused deposition modelling 3D printing is an increasingly utilized technology (*73*, *74*) which allows the rapid construction of 3D models with materials with varying mechanical properties. It enables durable 3D parts to be produced with a high accuracy and repeatability whilst allowing different components of a model to be printed with varying Young's moduli by blending the base materials. This method allows printing of complex CAD models, such as the anthropomorphic hand, in a single print where all parts of model are fused together. Support material is required to achieve functional compliant joints and ligaments structures which must be removed in post-processing step by removing chemically. The material used for each component of the CAD model can be determined individually, allowing the material properties of the ligaments to be varied individually; modulating the range and dynamic behavior of the hand.

A Stratasys Connex 5000 3D printer was used. Vero White, a photopolymer with high strength (tensile strength 60-70 MPa) and stiffness (flexile strength 75-110 MPa) was used to print the rigid bone structures (*75*). Vero white can be blended with other lower stiffness materials to print plastic with variable stiffness. In particular, it can be blended with Tango Black, which simulates thermoplastic elastomers with flexible, rubber-like qualities, with a Shore Hardness in the range of 26-28 Scale A, allowing up to 220% elongation at break. The ligaments were printed with the Tango Black Material blended with varying ratios of Vero White. The properties of the blends of materials used for the experiments are given in Table S1. The printing process takes approximately ten hours, with a further four required for effective mechanical and chemical removal of the support material. This allows rapid iteration of hand designs with minimal manual post-processing required. The hand can then be attached to a UR5 robot arm (Fig. 2) to allow wrist actuation and control. 3D printing allows the rapid and repetitive production of hand mechanical structures where the passive dynamic behaviors can be tailored, with minimal additional construction or development work required.

### *Experimental Setup*

For the experiments conducted in this article, the 3D printed hand skeletons were mounted directly on a UR5 robot arm. Using the arm allows precise static and dynamic control of the hand skeleton, allowing focus on the wrist kinematics without consideration for the rest of the arm. The on-board inverse kinematic of the UR5 is used, with a Python API used to allow control of the position, movement between poses and speed. The acceleration and deceleration of movement can be controlled in addition to the steady state speed allowing the dynamic and frequency response of the system to be measured. Positions corresponding to keyboard positions and fixed trajectories for chord jumps and thumb abduction movements have been collated into a database. Within this, the correct control parameters (speed, range of movement, frequency) are set to achieve the music required with the correct playing style for a specific material property required. More details of control parameters of the arm can be found in Supplementary Materials with a block diagram of the system given in Fig. S3.

To measure the details of the hand skeleton behaviors, and a ground truth of human playing, the piano was sensorized with force sensing resistors (FRS). A load cell was used to perform calibration of the sensors. Analogue digital converters on an Arduino microcontroller were used to register the response from these sensors in real time, while the data are synchronized with the arm motion commands.

### *Mechanical Characterization Experiments*

For the experiments investigating the single note playing behavior primitive (Fig. 4A), the playing of a single key instrumented with a force sensitive resistor was investigated. The index finger was used in the experiments, with differing ligament material ($E_J$) for the distal interphalangeal joint, proximal interphalangeal joint and metacarpophalangeal joints varied. For these experiments a single finger was used to allow the properties of the finger to be isolated from that of the rest of the hand as finger properties are determined only by $E_J$. The wrist control parameters (frequency, speed, displacement stroke distance) were varied for the different experiments and the response for the FSR on the key measured. The frequency of the force sensor signal was determined by measuring the average period of the output note as determined from the force sensor response, with the rate of changed used for the dynamic response. The maximum achieved force was used to indicate the achievable volume of playing. A range of frequencies, volumes and playing rates were chosen to map to typical human values and be within the capabilities of the arm providing the wrist actuation. All experiments were repeated five times with the average given.

For the thumb abduction experiments the ligament stiffness surrounding the joint ($E_J$) was varied keeping ligaments in the rest of the hand maintained at the lowest stiffness. Although the other joints, in particular the finger joints, contribute to the measured abduction this is minimal and kept constant across all experiments. The wrist is moved such that the thumb is playing a note (middle C) with a fixed downwards displacement and angle of inflection with the piano to allow sideways movement of the fingers. The wrist is then moved horizontal such that the thumb movement is limited by the key which it is pressing, exposing the movement of the fingers relative to the thumb. Using a camera fixed above the piano, the horizontal displacement between the thumb tip and the tip of the first finger the displacement can be measured. This was repeated five times, with the average distance recorded.

The final characterization is related to the hand span behavior primitive, with the material properties $E_S$ varied. Similarly, the remaining joint materials were maintained at the lowest stiffness. The second finger was moved downwards such that is pressing the middle C key. The wrist is then moved horizontal with the second finger trapped. The distance between the second and third finger is measured to provide a measurement of the compliance of the hand span. Finally, to investigate how this span stiffness affects the playing behavior the wrist is rotated and the little finger used to play notes with a fixed vertical displacement of 15mm, with the key force measured with a force sensitive resistor.

### *Piano Playing Experiments with Integrated Hand Skeleton*

The three excerpts of music were chosen based on the variety of playing modes as well as the three behavior primitives investigated in Fig. 4. For each phrase of music, the wrist location and movements were determined from the note requirements. For each piece of

music, the optimum material properties, and control parameters to achieve the playing style were chosen from the results shown in Fig. 4. More details of control parameters for the arm can be found in Supplementary Materials.

For registering the experimental data, the same force sensitive resistors were used on the piano keys. One, two, and three sensors were installed to obtain Fig. 5A, B, and C, respectively.

## SUPPLEMENTARY MATERIALS

**Fig. S1.** Hand CAD model showing the Finger ligament designs.
**Table S1. 3D Printer Materials** used and their material properties.
**Fig. S2. Full experimental setup**
**Fig. S3. Block diagram of the system for piano playing**
**Fig. S4. Experimental Method for determine the compliance of a single finger.**
**Table S2. Summary of Arm control parameters.**
**Fig. S5. Toccata music separated into regions.**
**Fig. S6. Flow chart of the motion planning required for playing Toccata**
**Fig. S7. Alligator Crawl.**
**Fig. S8. Flow chart for Alligator Crawl.**
**Table S4. Summary of Arm parameters used in the arm control for playing Toccata.**
**Fig. S9. Adapted music for Rhapsody in blue and motion planning flowchart.**
**Table S5. Summary of Arm parameters used in the arm control for playing Rhapsody in Blue.**

**Movie S1. Fabrication.** Video showing a time lapse of the 3D printing process for the hand showing how a hand can be printed in a single prin. This demonstrates the flexibility of the hand once produced and the passive dynamics.
**Movie S2. Single Finger Behavior.** Shows the range of movement of a single finger and the response from fingers of different stiffness when provided with the same vertical movement to play a single note showing the variation in resultant morphology and also output sound.
**Move S3. Abduction/Adduction Behavior.** Demonstrates abduction and adduction behavior of a single hand and the range of piano playing this enables.
**Movie S4. Hand span Playing Behavior.** Playing with the hand at angles allows jumps of various intervals to be made.
**Movie S5. Three Pieces of Music Playing.** Using a single 3D printed hand to play music of different styles and forms. Recorded using a single camera, this shows a compilation of different experimental repeats of the experiment from different angles.

## References and Notes


1. S. Kim, C. Laschi, B. Trimmer, Soft robotics: a bioinspired evolution in robotics. *Trends Biotechnol.* **31**, 287–294 (2013).
2. R. Pfeifer, M. Lungarella, F. Iida, The challenges ahead for bio-inspired “soft” robotics. *Commun. ACM*. **55**, 76 (2012).
3. M. Calisti *et al.*, An octopus-bioinspired solution to movement and manipulation for soft robots. *Bioinspir. Biomim.* **6**, 36002 (2011).
4. R. Pfeifer, M. Lungarella, F. Iida, Self-organization, embodiment, and biologically inspired robotics. *Science*. **318**, 1088–93 (2007).
5. A. Jan Ijspeert, A. Crespi, D. Ryczko, J.-M. Cabelguen, From Swimming to Walking with a Salamander Robot Driven by a Spinal Cord Model. *Science (80-. ).* **315**, 1416–1420 (2007).
6. R. Pfeifer, F. Iida, M. Lungarella, Cognition from the bottom up: on biological inspiration, body morphology, and soft materials. *Trends Cogn. Sci.* **18**, 404–413 (2014).
7. D. N. Beal, F. S. Hover, M. S. Triantafyllou, J. C. LIao, G. V. Lauder, Passive propulsion in vortex wakes. *J. Fluid Mech.* **549**, 385–402 (2006).
8. T. Hatanaka, N. Chopra, M. W. Spong, in *2015 54th IEEE Conference on Decision and*

*Control (CDC)* (IEEE, 2015), pp. 2450–2452.
9. S. Collins, A. Ruina, R. Tedrake, M. Wisse, Efficient bipedal robots based on passive-dynamic walkers. *Science*. **307**, 1082–5 (2005).
10. F. Boyer, M. Porez, F. Morsli, Y. Morel, Locomotion Dynamics for Bio-inspired Robots with Soft Appendages: Application to Flapping Flight and Passive Swimming. *J. Nonlinear Sci.* **27**, 1121–1154 (2017).
11. I. Fantoni, R. Lozano, M. W. Spong, Energy based control of the Pendubot. *IEEE Trans. Automat. Contr.* **45**, 725–729 (2000).
12. Guilin Yang, I-Ming Chen, Wei Lin, J. Angeles, Singularity analysis of three-legged parallel robots based on passive-joint velocities. *IEEE Trans. Robot. Autom.* **17**, 413–422 (2001).
13. F. L. Hammond, J. Weisz, A. A. de la Llera Kurth, P. K. Allen, R. D. Howe, in *2012 IEEE International Conference on Robotics and Automation* (IEEE, 2012), pp. 2843–2850.
14. L. U. Odhner, R. R. Ma, A. M. Dollar, Open-Loop Precision Grasping With Underactuated Hands Inspired by a Human Manipulation Strategy. *IEEE Trans. Autom. Sci. Eng.* **10**, 625–633 (2013).
15. I. Poulakakis, E. Papadopoulos, M. Buehler, On the Stability of the Passive Dynamics of Quadrupedal Running with a Bounding Gait. *Int. J. Rob. Res.* **25**, 669–687 (2006).
16. J.-B. Mouret, S. Doncieux, Encouraging Behavioral Diversity in Evolutionary Robotics: An Empirical Study. *Evol. Comput.* **20**, 91–133 (2012).
17. N. Ulrich, R. Paul, R. Bajcsy, in *Proceedings. 1988 IEEE International Conference on Robotics and Automation* (IEEE Comput. Soc. Press; http://ieeexplore.ieee.org/document/12087/), pp. 434–436.
18. A. M. Dollar, R. D. Howe, The Highly Adaptive SDM Hand: Design and Performance Evaluation. *Int. J. Rob. Res.* **29**, 585–597 (2010).
19. M. T. Mason, A. Rodriguez, S. S. Srinivasa, A. S. Vazquez, Autonomous manipulation with a general-purpose simple hand. *Int. J. Rob. Res.* **31**, 688–703.
20. H. Arai, S. Tachi, Position control of manipulator with passive joints using dynamic coupling. *IEEE Trans. Robot. Autom.* **7**, 528–534 (1991).
21. B. Roy, H. H. Asada, Nonlinear Feedback Control of a Gravity-Assisted Underactuated Manipulator With Application to Aircraft Assembly. *IEEE Trans. Robot.* **25**, 1125–1133 (2009).
22. D. Aukes, S. Kim, P. Garcia, A. Edsinger, M. R. Cutkosky, in *2012 IEEE International Conference on Robotics and Automation* (IEEE, 2012; http://ieeexplore.ieee.org/document/6224738/), pp. 2824–2829.
23. L. U. Odhner *et al.*, A compliant, underactuated hand for robust manipulation. *Int. J. Rob. Res.* **33**, 736–752 (2014).
24. G. Grioli, M. Catalano, E. Silvestro, S. Tono, A. Bicchi, in *2012 IEEE/RSJ International Conference on Intelligent Robots and Systems* (IEEE, 2012; http://ieeexplore.ieee.org/document/6385881/), pp. 1251–1256.
25. S. Wolf, G. Hirzinger, in *2008 IEEE International Conference on Robotics and Automation* (IEEE, 2008; http://ieeexplore.ieee.org/document/4543452/), pp. 1741–1746.
26. A. Albu-Schaffer *et al.*, Soft robotics. *IEEE Robot. Autom. Mag.* **15**, 20–30 (2008).
27. S. Wolf *et al.*, Variable Stiffness Actuators: Review on Design and Components. *IEEE/ASME Trans. Mechatronics*. **21**, 2418–2430 (2016).
28. S. Haddadin, F. Huber, A. Albu-Schaffer, in *2012 IEEE International Conference on Robotics and Automation* (IEEE, 2012; http://ieeexplore.ieee.org/document/6225190/), pp. 3347–3354.
29. G. Palli, C. Melchiorri, in *Advanced Robotics, 2009. ICAR 2009. International Conference on* ([IEEE], Munich, 2009).

30. J. Z. Wu, Z.-M. Li, R. G. Cutlip, K.-N. An, A simulating analysis of the effects of increased joint stiffness on muscle loading in a thumb. *Biomed. Eng. Online*. **8**, 41 (2009).
31. M. Manti, V. Cacucciolo, M. Cianchetti, Stiffening in Soft Robotics: A Review of the State of the Art. *IEEE Robot. Autom. Mag.* **23**, 93–106 (2016).
32. N. Correll, C. Heckman, Materials that make robots smart (available at https://arxiv.org/pdf/1711.00537.pdf).
33. A. Jiang, G. Xynogalas, P. Dasgupta, K. Althoefer, T. Nanayakkara, in *2012 IEEE/RSJ International Conference on Intelligent Robots and Systems* (IEEE, 2012; http://ieeexplore.ieee.org/document/6385696/), pp. 2922–2927.
34. J. Nagase, S. Wakimoto, T. Satoh, N. Saga, K. Suzumori, Design of a variable-stiffness robotic hand using pneumatic soft rubber actuators. *Smart Mater. Struct.* **20**, 105015 (2011).
35. F. Ilievski, A. D. Mazzeo, R. F. Shepherd, X. Chen, G. M. Whitesides, Soft Robotics for Chemists. *Angew. Chemie*. **123**, 1930–1935 (2011).
36. J. Hughes *et al.*, Soft Manipulators and Grippers: A Review. *Front. Robot. AI*. **3**, 69 (2016).
37. D. Trivedi, C. D. Rahn, W. M. Kier, I. D. Walker, Soft robotics: Biological inspiration, state of the art, and future research. *Appl. Bionics Biomech.* **5**, 99–117 (2008).
38. A. Bicchi, G. Tonietti, Fast and "Soft-Arm" Tactics. *IEEE Robot. Autom. Mag.* **11**, 22–33 (2004).
39. M. Cianchetti *et al.*, Soft Robotics Technologies to Address Shortcomings in Today's Minimally Invasive Surgery: The STIFF-FLOP Approach. *Soft Robot.* **1**, 122–131 (2014).
40. M. G. Catalano *et al.*, in *2011 IEEE International Conference on Robotics and Automation* (IEEE, 2011; http://ieeexplore.ieee.org/document/5980457/), pp. 5090–5095.
41. C. Della Santina *et al.*, Postural Hand Synergies during Environmental Constraint Exploitation. *Front. Neurorobot.* **11**, 41 (2017).
42. M. Santello *et al.*, Hand synergies: Integration of robotics and neuroscience for understanding the control of biological and artificial hands. *Phys. Life Rev.* **17**, 1–23 (2016).
43. M. G. Catalano *et al.*, (Springer, Cham, 2016; http://link.springer.com/10.1007/978-3-319-26706-7_8), pp. 101–125.
44. F. J. Valero-Cuevas *et al.*, The Tendon Network of the Fingers Performs Anatomical Computation at a Macroscopic Scale. *IEEE Trans. Biomed. Eng.* **54**, 1161–1166 (2007).
45. N. W. Bartlett *et al.*, SOFT ROBOTICS. A 3D-printed, functionally graded soft robot powered by combustion. *Science*. **349**, 161–5 (2015).
46. D. Rus, M. T. Tolley, Design, fabrication and control of soft robots. *Nature*. **521**, 467–475 (2015).
47. T. Umedachi, V. Vikas, B. A. Trimmer, in *2013 IEEE/RSJ International Conference on Intelligent Robots and Systems* (IEEE, 2013; http://ieeexplore.ieee.org/document/6697016/), pp. 4590–4595.
48. G. Salvietti, Replicating human hand synergies onto robotic hands: A review on software and hardware strategies. *Front. Neurorobot.* **12**, 1–6 (2018).
49. Z. Xu, V. Kumar, Y. Matsuoka, E. Todorov, Design of an Anthropomorphic Robotic Finger System with Biomimetic Artificial Joints (available at https://pdfs.semanticscholar.org/b36d/a023cd0c898c39cc3919573f81ae9e9629fe.pdf).
50. S. H. Jeong, K. Kim, S. Kim, Designing Anthropomorphic Robot Hand with Active Dual - Mode Twisted String Actuation Mechanism and Tiny Tension Sensors. *Ieee Robot. Autom. Lett.* **3766**, 1–8 (2017).
51. N. Thayer, S. Priya, Design and implementation of a dexterous anthropomorphic robotic typing (DART) hand. *Smart Mater. Struct.* **20** (2011), doi:10.1088/0964-

1726/20/3/035010.
52. Eppner, Clemens, et al., Exploitation of environmental constraints in human and robotic grasping. *IJRR. 34*(7), 1021-1038
53. D. D. Damian, T. H. Newton, R. Pfeifer, A. M. Okamura, Artificial Tactile Sensing of Position and Slip Speed by Exploiting Geometrical Features. *IEEE/ASME Trans. Mechatronics*. **20**, 263–274 (2015).
54. B. H. Kang, J. T. Wen, N. G. Dagalakis, J. J. Gorman, Analysis and design of parallel mechanisms with flexure joints. *IEEE Trans. Robot.* **21**, 1179–1185 (2005).
55. S. H. Ahn *et al.*, Smart Soft Composite: An Integrated 3D Soft Morphing Structure Using Bend-twist Coupling of Anisotropic Materials. *Int. J. Precis. Eng. Manuf.* **13**, 631–634 (2012).
56. R. B. Gillespie, B. Yu, R. Grijalva, S. Awtar, Characterizing the Feel of the Piano Action. *Comput. Music J.* **35**, 43–57 (2011).
57. S. Sugano, I. Kato, in *Proceedings. 1987 IEEE International Conference on Robotics and Automation* (Institute of Electrical and Electronics Engineers; http://ieeexplore.ieee.org/document/1088025/), vol. 4, pp. 90–97.
58. Y.-F. Li, Chi-Yi Lai, in *2014 IEEE 23rd International Symposium on Industrial Electronics (ISIE)* (IEEE, 2014; http://ieeexplore.ieee.org/document/6864843/), pp. 1538–1543.
59. D. Zhang, Jianhe Lei, Beizhi Li, D. Lau, C. Cameron, in *2009 International Conference on Information and Automation* (IEEE, 2009; http://ieeexplore.ieee.org/document/5205022/), pp. 757–761.
60. V. Jaju, A. Sukhpal, P. Shinde, A. Shroff, A. B. Patankar, in *2016 International Conference on Internet of Things and Applications (IOTA)* (IEEE, 2016; http://ieeexplore.ieee.org/document/7562726/), pp. 223–226.
61. J.-C. Lin, H.-H. Huang, Y.-F. Li, J.-C. Tai, L.-W. Liu, in *2010 International Symposium on Computer, Communication, Control and Automation (3CA)* (IEEE, 2010; http://ieeexplore.ieee.org/document/5533457/), pp. 353–356.
62. C. Borst, M. Fischer, S. Haidacher, H. Liu, G. Hirzinger, in *2003 IEEE International Conference on Robotics and Automation (Cat. No.03CH37422)* (IEEE; http://ieeexplore.ieee.org/document/1241676/), vol. 1, pp. 702–707.
63. A. Gustus, G. Stillfried, J. Visser, H. Jörntell, P. van der Smagt, Human hand modelling: kinematics, dynamics, applications. *Biol. Cybern.* **106**, 741–755 (2012).
64. Y. Zhang, H. Deng, G. Zhong, Humanoid design of mechanical fingers using a motion coupling and shape-adaptive linkage mechanism. *J. Bionic Eng.* **15**, 94–105 (2018).
65. D. Burke, S. C. Gandevia, G. Macefield, Responses to passive movement of receptors in joint, skin and muscle of the human hand. *J. Physiol.* **402**, 347–361 (1988).
66. P. E. Klopsteg *et al.*, The Anatomy and Mechanics of the Human Hand (1955) (available at http://www.oandplibrary.net/al/pdf/1955_02.pdf#page=26).
67. C. C. Norkin, D. J. White, R2 Library (Online service), *Measurement of joint motion : a guide to goniometry*.
68. A. Hollister *et al.*, The Axes of Rotation of the Thumb Interphalangeal and Metacarpophalangeal Joints. *Clin. Orthop. Relat. Res. Number*. **320** (1995).
69. D. C. Harding, K. D. Brandt, B. M. Hillberry, Finger joint force minimization in pianists using optimization techniques. *J. Biomech.* **26**, 1403–12 (1993).
70. K. C. Engel, M. Flanders, J. F. Soechting, Anticipatory and sequential motor control in piano playing. *Exp. Brain Res.* **113**, 189–199 (1997).
71. M. Chalon, M. Grebenstein, T. Wimböck, G. Hirzinger, in *2010 IEEE/RSJ International Conference on Intelligent Robots and Systems* (IEEE, 2010; http://ieeexplore.ieee.org/document/5650454/), pp. 5886–5893.
72. S. Furuya, M. Flanders, J. F. Soechting, Hand kinematics of piano playing. *J.*

*Neurophysiol.* **106**, 2849–2864 (2011).
73. R. L. Truby, J. A. Lewis, Printing soft matter in three dimensions. *Nature*. **540**, 371–378 (2016).
74. M. Wehner *et al.*, An integrated design and fabrication strategy for entirely soft, autonomous robots. *Nature*. **536**, 451–455 (2016).
75. Vero, (available at http://www.stratasys.com/materials/search/vero).

## Acknowledgments

**Funding:** This work was funded by The United Kingdom Engineering and Physical Sciences Research Council (EPSRC) MOTION grant [EP/N03211X/2] and the EPSRC CDT in Sensor Technologies (Grant EP/L015889/1).. **Author contributions**: J.H. designed and performed all experiments; J.H, F.I and P.M wrote the paper. **Data and materials availability**: All (other) data needed to evaluate the conclusions in the paper are present in the paper or the Supplementary Materials.

# Supplementary Materials

## CAD, Hand Design and 3D Printing

The hand has been designed using an anthropomorphic hand model, which has then been adapted using the CAD software 3DS Max. The ligament design has been simplified to reduce the number of variables, with the joints modelled as ellipse shells (Fig. S1). The shell thickness has been designed such that the ligaments are sufficiently strong to prevent ripping or tearing and prevent weakness of the joint.

The 3D printer used is a Stratasys Connex 5000, which prints the material in layers, with UV light used to cure the liquid material deposited. This requires a solid model to be produced, with support material printed in locations where there is not material, for example within he ligaments shells in the areas where bones interact. To remove the support material from inside the joints there must be access for the chemical solvent used, and thus small relief holes are used in the undersides of the joints (Fig. S1.)

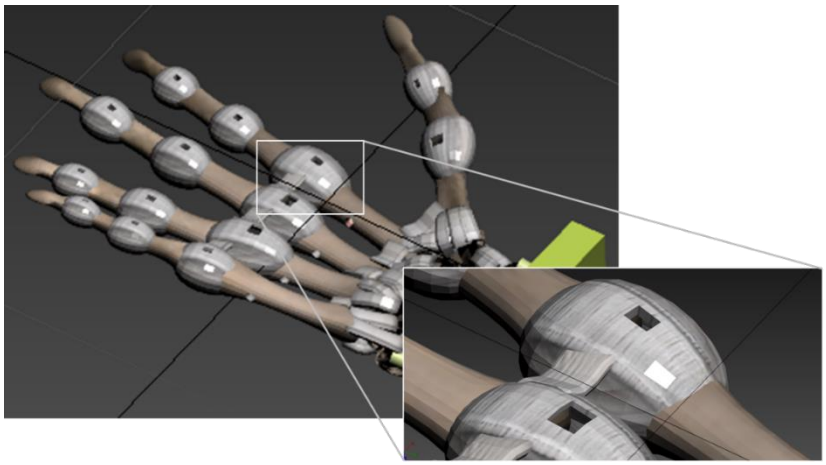

**Fig. S1.** Hand CAD model showing the finger joint design, with the inset picture showing how the softer ligament material has square cut outs to allow the support material to be removed from the joint area after printing.

The different blends of materials and the properties used are shown in Table S1. There are four different ligament materials with varying blends of Tango Black and rigid plastic which are used in experiments. The fused deposition 3D printing methods requires the use of support material in the fabrication such that the hand can be printed in layers. The support material must be removed from the hand using a combination of mechanical removal and chemical removal.

**Table S1. 3D Printer Materials used when printing the hand.** Includes the ligaments of different stiffnesses, and the bones. Shows the blend of blasé materials used to generate the materials with a given stiffness.

| | **Tango Black Percentage (%)** | **Agile White Percentage (%)** | **Shore Hardness** | **Young's Modulus (E)** |
|---|---|---|---|---|
| Ligament (least stiff) | 100 | 0 | A97 | 1 MPa |
| Ligaments | 90 | 10 | A75 | 2.5 MPa |
| Ligaments | 80 | 20 | A50 | 20 MPa |
| Ligaments (most stiff) | 70 | 30 | A25 | 50 MPa |
| Bones | 0 | 100 | - | 2GPa |

## Experimental Setup

The full experimental setup is shown in Fig. S2. A UR5 robot, which offers 6 degrees of freedom, is used to provide the wrist actuation. The 3D printed hand is mounted securely on the end of the arm using bolts.

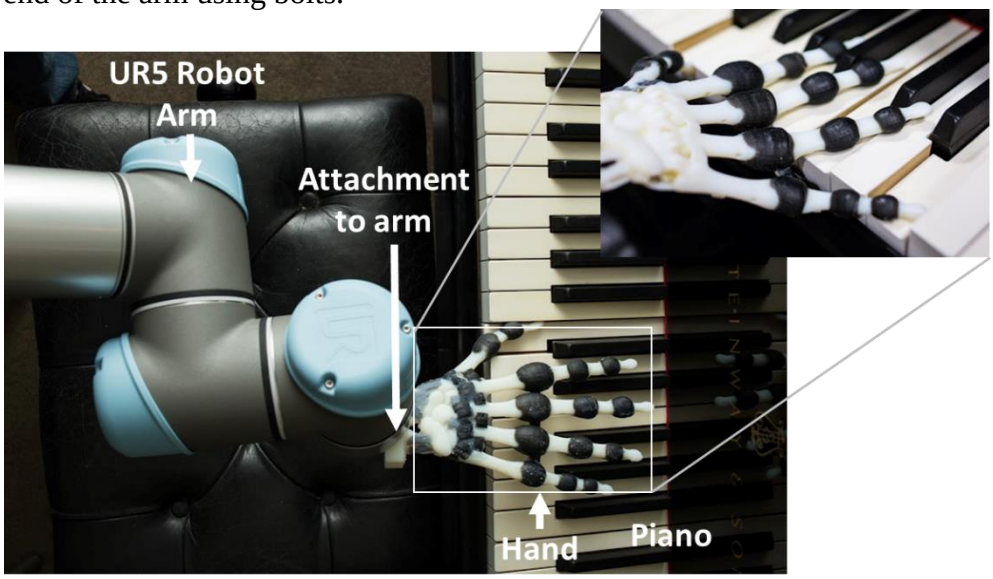


**Fig. S2. Full experimental setup showing the UR5 Arm.** The attachment of the hand to the arm and the 3D printed hand. The UR5 arm is placed such that it is perpendicular to the environment, which is in this case the piano.

A block diagram of the implementation of piano playing is shown in Fig. S3. The inputs (music, mechanical properties, environmental properties and a database of known note locations and transitions) are input into a planner, which determines the control parameters and required locations. The UR5 arm controller is used to determine the inverse kinematics and then control the UR5 Arm. This allows the hand to be moved relative to the environment, with the Conditional Stiffness, giving rise to output behavior in the form of piano playing.

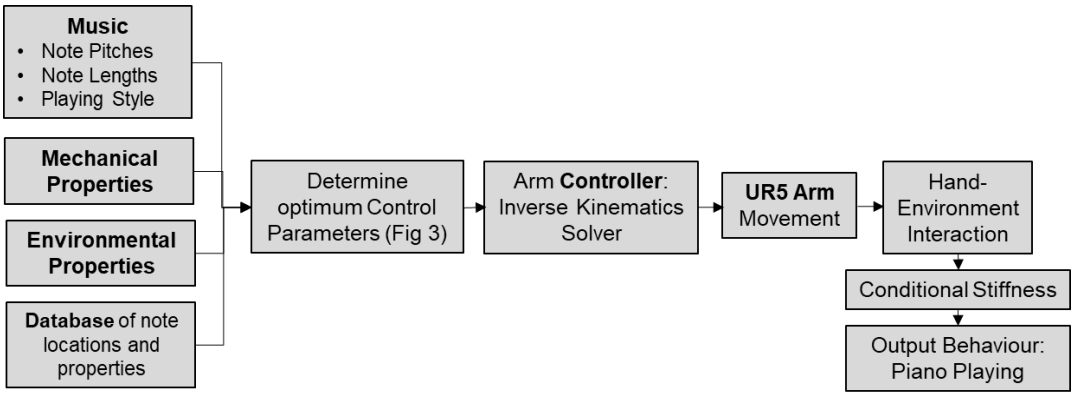


**Fig. S3. Block diagram of the system for piano playing.** Showing the inputs, planning system and the overall output, piano playing.

## Anisotropic Hand Stiffness

### *Experimental Methods*

To measure the compliance of stiffness of the individual finger, the finger was mounted in a fixed position horizontally. A known force is then applied to the finger-tip, and the displacement between the center line of the finger and the displaced finger tip-measured. This method is shown in Fig. S4. The compliance of the finger can then be determined:

$$Compliance_{angle} = \frac{Force\ Applied}{\Delta z}$$

This method can be extended to investigating the directional stiffness of the thumb joint and also the finger joints around other planes of rotation.

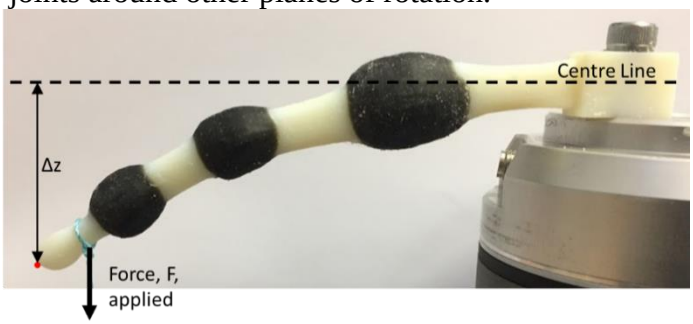


**Fig. S4. Experimental method for measuring the compliance of a single finger.** The three joints of the finger are used, with the finger fixed at a given orientation. A force is applied with the displacement of the finger tip in the direction of the force measured.

### *Passive Hand Compliance*

The thumb is particularly complex due to the ability of the thumb joint to distend, and the complex network of ligaments used to construct the joints gives rise to stiffness, which is highly direction.

The 3D printer materials, blends of materials and their used shore hardness and Young's Modulus is shown in Table S1. Three behavior primitives are presented in this paper: single note playing, thumb abduction and chord spreading. These behavior primitives form the basis of many different hand playing morphologies and structures.

## Arm Actuation

Inverse kinematics of the UR5 is used to allow control of the end effector in Cartesian co-ordinates. The considered control parameters include the position of the end effector and the corresponding velocities:

$$W = \begin{bmatrix} x & y & z \\ \alpha & \beta & \gamma \end{bmatrix}$$

$$\dot{W} = \begin{bmatrix} \dot{x} & \dot{y} & \dot{z} \\ \dot{\alpha} & \dot{\beta} & \dot{\gamma} \end{bmatrix}$$

We consider the following parameters for the corresponding elements of piano playing:

**Table S2. Summary of Arm control parameters.** The dependency of wrist parameters on playing behaviour and the dependency of this on material hand properties.

| Music Playing Behaviour | Wrist Parameters | Dependency on Hand Properties |
|---|---|---|
| Note pitch (note location) | x,y | - |
| Note length | T | - |
| Articulation (legato/staccato) | $\dot{z}$ | $E_J$ |

| | | |
|---|---|---|
| Volume | $\Delta z$ | $E_J$ |
| Abduction/Adduction distance | $\Delta x,$ | $E_T$ |
| Single Finger span movement | $\Delta x$ | $E_S$ |
| Angled Hand Playing | $\alpha$ | $E_S$ |

The specific arm actuation and motion planning used for the three pieces played, are summarized in the following section with the motion planning represented in a flow chart with the specific actuation principles provided which corresponding to the elements in Table S2.

***Toccata, Scarlatti***

Requires the repeated staccatto playing using the **third finger** with has a stiffness **$E_J$ of 50MPa**.

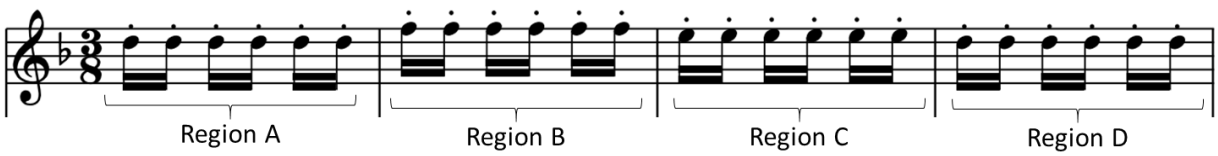


**Fig. S5. Toccata music separated into regions.** The 4 different regions of the music which have different playing positions.

The motion planning is summarized by the flow chart in Fig. S6. with the corresponding parameters given in Table S3. For the twenty experimental repetitions of the playing there was 100% in the hand performing the piece, with no piano keys missed.

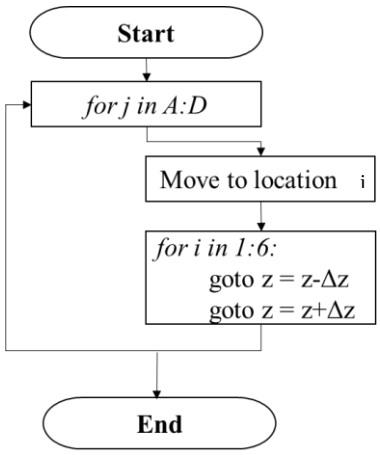


**Fig. S6. Flow chart of the motion planning required for playing Toccata.** Repeated note playing a the four different locations.

**Table S3. Summary of arm parameters used in the arm control for playing Toccata.**

| **Music Playing Behaviour** | **Wrist Parameters** | **Values** |
|---|---|---|
| Note pitch (note location) | Starting Location, Region (A) (x,y,z)<br>Region (B) (x + 27,y,z)<br>Region (C) (x + 13.5,y,z)<br>Region (D) (x,y,z) | "x": -78.18,<br>"y": -81.50,<br>"z": 120.22 |
| Articulation (legato/staccato) | $\dot{z}$ | 0.25m/s |

| | | |
|---|---|---|
| Volume | $\Delta z$ | 15mm |

***Alligator Crawl, Fats Waller***

The Alligator Crawl music uses two fingers for playing, the thumb and little finger. The thumb is used to play the lower note and then the little finger the higher note in each pair. There are five different locations (A-D) in which the pattern is repeated. The thumb stiffness, $E_J$, is low to help enable travelling between the two notes, as is the span stiffness. The little finger is angled to help achieve sufficient force when playing. For the twenty experimental repetitions, due to the accumulation of erroring the drift of position of the arm, of the many times the little finger was used to play the higher notes, in 4% of cases, there was a mis-played note.

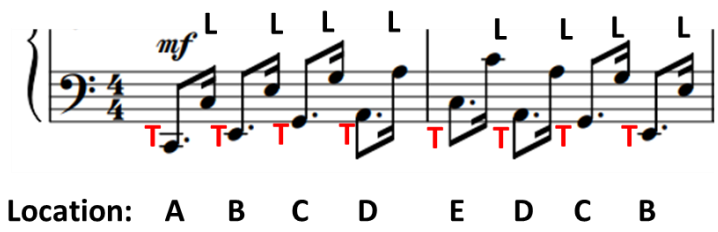


**Fig. S7. Alligator Crawl.** Showing which fingers are used to play different notes (thumb, 'T', or little finger, 'L') with different locations, which are repeated throughout the musical phrase.

The flow chart summarizing the motion planning for playing Alligator Crawl is given in Fig. S10.

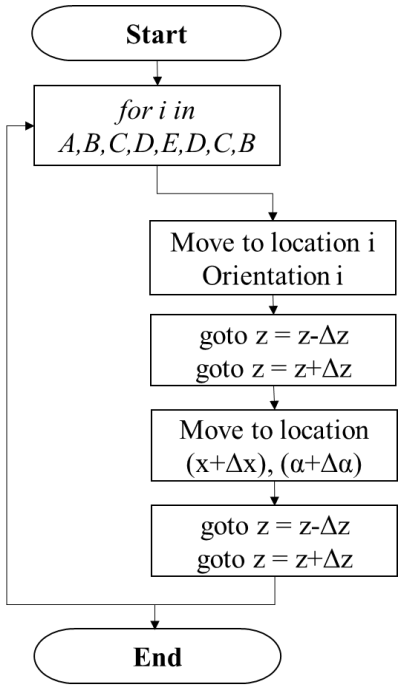


**Fig. S8. Flow chart for Alligator Crawl.** Shows the motion planning for the sequence. Corresponds to Table S4, which specifies the specific magnitudes.

Minor manual adjustment of the motion plan was required – in particular when stepping down note locations (e.g. when travelling from locations E-D-C-B).

**Table S4. Summary of arm parameters used in the arm control for playing Toccata.**

| Music Playing behavior | Wrist Parameters | Values |
|---|---|---|

| | | |
|---|---|---|
| Note pitch (note location) | Starting Location, (A) (x,y,z,α)<br>B=(x+27,y,z)<br>C=(x+54,y,z)<br>D=(x+81,y,z)<br>E=(x+108,y,z) | "x": -72.93,<br>"y": -67.50,<br>"z": 130.29, |
| Articulation (legato/staccato) | $\dot{z}$ | $0.2m/s$ |
| Volume | $\Delta z$ | 17mm |
| Abduction/Adduction distance | $\Delta x,$ | ~5mm |
| Single Finger span movement | $\Delta x$ | ~5mm |
| Angled Hand Playing | $\alpha$ | Thumb = -5°<br>Little Finger 35° |

***Rhapsody in Blue, Gershwin***

Rhapsody in Blue is all played with the thumb, with the abduction of the thumb used to allow smooth glissando playing between notes. For the twenty experimental repetitions of the playing there was 100% in the hand performing the piece, with no piano keys missed.

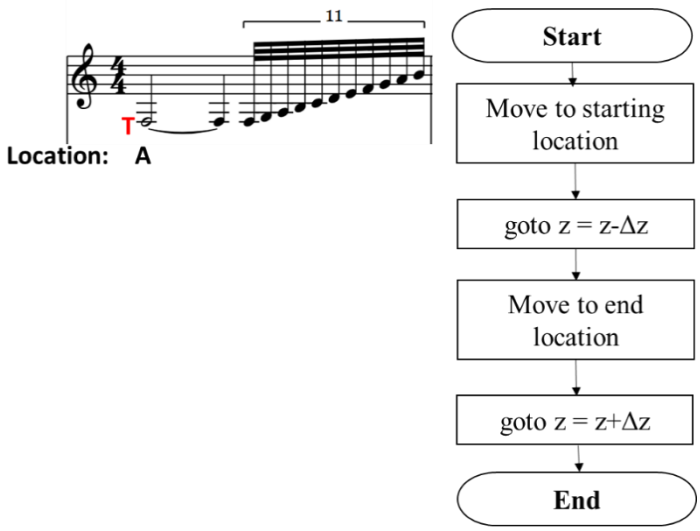


**Fig. S9. Adapted music for Rhapsody in blue and motion planning flowchart.** Shows the motion planning for the sequence, with the specific values of parameters given in Table S5.

**Table S5. Summary of arm parameters used in the arm control for playing Rhapsody in Blue.**

| Music Playing Behavior | Wrist Parameters | Values |
|---|---|---|
| Note pitch (note location) | Starting Location: (x,y,z α)<br>End location: (x,y,z α) | "x": -72.93,<br>"y": -67.50,<br>"z": 130.29, |
| Volume | $\Delta z$ | 17mm |
| Abduction/Adduction distance | $\Delta x,$ | ~5mm |

## Video Files

**Movie S1. Fabrication.** Video showing a time lapse of the 3D printing process for the hand showing how a hand can be printed in a single prin. Shows the flexibility of the hand once produced and the passive dynamics.

**Movie S2. Single Finger Behavior.** Shows the range of movement of a single finger and the response from fingers of different stiffness when provided with the same vertical movement to play a single note showing the variation in resultant morphology and also output sound.

**Move S3. Abduction/Adduction Behavior.** Demonstrates abduction and adduction behavior of a single hand and the range of piano playing this enables.

**Movie S4. Hand span Playing Behavior.** Playing with the hand at angles allows jumps of various intervals to be made.

**Movie S5. Three Pieces of Music Playing.** Using a single 3D printed hand to play music of different styles and forms. Show different camera views from different repeats of the experiment.